

Self-dual solitons in a Maxwell-Chern-Simons baby Skyrme model

Rodolfo Casana,^{*} André C. Santos,[†] Claudio F. Farias,[‡] and Aleksandro L. Mota[§]
Departamento de Física, Universidade Federal do Maranhão, 65080-805, São Luís, Maranhão, Brazil.

We have studied the existence of self-dual solitons in a gauged version of the baby Skyrme model in which the gauge field dynamics is governed by the Maxwell-Chern-Simons action. For such a purpose, we have developed a detailed implementation of the Bogomol'nyi-Prasad-Sommerfield formalism providing the self-dual equations whose solutions saturate the energy lower bound. Such a bound related to the topological charge of the Skyrme field becomes quantized whereas both the total magnetic flux and the total electrical charge are not. We have found two types of self-dual Skyrme field profiles: the first is described by a solution which decays following an exponential-law ($e^{-\alpha r^2}$, $\alpha > 0$); the second is portrayed by a solution having a power-law decay ($r^{-\beta}$, $\beta > 0$). On the other hand, in both cases the asymptotic behavior of the gauge field is similar to the one presented in the context of the Abelian Higgs models describing Abrikosov-Nielsen-Olesen charged vortices. Other interesting feature we highlight is the localized magnetic flux inversion, a property not observed in other gauged baby Skyrme models already studied in literature. Numerical results are presented for rotationally symmetrical field configurations by remarking some of its essential features.

I. INTRODUCTION

The Skyrme model [1] is a non-linear field theory, which is originally defined in $(3 + 1)$ dimensions and whose soliton solutions are called Skyrmions, it has been a prolific subject in several branches of physics. Initially, it was proposed as an effective field theory for nuclear phenomena that avoid some technical difficulties present in its underlying theory, more specifically the Quantum Chromodynamics. This model was reasonably successful in obtaining several hadrons and nucleons properties [2–5], with the latter emerging as topological soliton solutions called Skyrmions. Further, recently it has found an exciting research field in the realm of condensed matter physics. The Skyrme model has been studied for physical systems such as liquid Helium [6, 7], quantum hall effect [8–10], Bose-Einstein condensates [11] and chiral nematic liquid crystals [12]. However, most promising results were found in magnetic materials [13–15] and superconductors [16–24]. The first one provides some theoretical and experimental realizations that can yield important technological applications such as data storage and spintronic.

The $(2 + 1)$ -dimensional version of the full model [1] is called baby Skyrme model [25] being described by the Lagrangian density

$$\mathcal{L} = \frac{\nu^2}{2} \partial_\mu \vec{\phi} \cdot \partial^\mu \vec{\phi} - \frac{\lambda^2}{4} (\partial_\mu \vec{\phi} \times \partial_\nu \vec{\phi})^2 - V(\phi_n). \quad (1)$$

The first contribution is the well-known nonlinear σ -model term. The second term is the counterpart of the Skyrme term in Ref. [1]. The last term, $V(\phi_n) \equiv V(\vec{n} \cdot \vec{\phi})$, is an appropriate self-interacting potential added with

aim to guarantee the stability of the soliton solutions [26]. The vector $\vec{\phi}$ is the Skyrme field denoting a triplet of real scalar fields $\vec{\phi} = (\phi_1, \phi_2, \phi_3)$ satisfying the constraint $\vec{\phi} \cdot \vec{\phi} = \phi_1^2 + \phi_2^2 + \phi_3^2 = 1$, which stands on a unit two-sphere (denoted by \mathbb{S}^2), and the unitary vector $\vec{n} \in \mathbb{S}^2$ provides a preferred direction in the internal space. The σ -model and Skyrme terms are invariant under the $SO(3)$ global symmetry whereas the potential breaks partially it but preserving the $U(1)$ subgroup. The potential has a unique vacuum configuration and must satisfy the condition $V(\phi_n) \rightarrow 0$ when $\phi_n \rightarrow 1$.

In absence of the σ -model term, the resulting is the named *restricted* baby Skyrme model which was firstly considered in Ref. [27]. The Bogomol'nyi structures [obtained via the Bogomol'nyi-Prasad-Sommerfield (BPS) formalism] in this model were investigated in Ref. [28], there has been found the energy lower bound (Bogomol'nyi limit or BPS bound) and the respective self-dual or BPS equations satisfied by the soliton configurations saturating such a bound.

A natural physical extension in the study of the baby Skyrme model is the possibility of its coupling to the electromagnetic field in order to investigate their electric and/or magnetic properties. It is achieved by promoting the $U(1)$ global symmetry to be a local gauge symmetry by means of the introduction of an Abelian gauge field, whose dynamics can be governed solely by the Maxwell term [29–32] or the Chern-Simons term [33], or also by both the Maxwell and the Chern-Simons terms [34–37].

Even though of investigations involving BPS structures in the gauged versions of the nonlinear σ -model (for example, when it is minimally coupled to the Maxwell term [38] or the Chern-Simons term [39], or still both the Maxwell and the Chern-Simons terms [40]) has been successful, similar results by applying the BPS formalism have never been obtained for a baby Skyrme model. Such a limitation can be partially circumvented by adopting gauged versions of the restricted baby Skyrme model.

^{*} rodolfo.casana@gmail.com

[†] andre_cavs@hotmail.com

[‡] cffarias@gmail.com

[§] lucenalexster@gmail.com

Thus, BPS solitons has been obtained in a gauged restricted model whose gauge field dynamics is governed by the Maxwell term [41]. All these results have inspired the development a wide range of applications, including topological phase transitions [30], Bogomol'nyi equations based in the strong necessary conditions limit [42], gauged BPS baby skyrmions with quantized magnetic flux [43] and even in supersymmetry [44–48] and gravitational theories [49].

Recently was well established the existence of self-dual configurations in a generalized Chern-Simons baby Skyrme model by means of a successful implementation of the BPS technique [33]. Further, in Refs. [34, 35] has been studied some properties of the solitonic solutions emerging in the Maxwell-Chern-Simons baby Skyrme model, nevertheless, still remains open the obtaining of self-dual solitons via direct application of the BPS formalism. On the other side, the existence of BPS structures in gauged baby Skyrme models including the Chern-Simons term also has been revealed by using supersymmetry techniques [48], specifically, these models possess $N = 2$ SUSY extension. The matching of the BPS structures arising via the direct use of the BPS technique and SUSY formalism in the Chern-Simons baby Skyrme model has been discussed in [33].

Our aim is the construction of a BPS description of the solitonic solutions (and their main features) emerging in a gauged baby Skyrme model whose gauge field dynamic is governed by the Maxwell-Chern-Simons action. The manuscript is divided as follows. In Secs. II and III, we present the essential features of the Maxwell-Chern-Simons restricted baby Skyrme model and the necessity to introduce an auxiliary dynamical field with the aim to gain a BPS model. Immediately, the developing of the BPS formalism provides the BPS potential, the self-dual equations and the Bogomol'nyi bound for the total energy. In Sec. IV, we restrict our analysis to the study of rotationally symmetric solutions by discussing the boundary conditions and obtaining the physical quantities, namely, the magnetic flux and the electrical charge. In Sec. V, we depict some relevant profiles and discuss their quantitative and qualitative features. In Sec. VI, we present our remarks and conclusions.

II. MAXWELL-CHERN-SIMONS RESTRICTED BABY SKYRME MODEL

The gauged version of the baby Skyrme model which consider the Skyrme field minimally coupled to the Maxwell-Chern-Simons field [34, 35] is described by the following Lagrangian density

$$L = E_0 \int d^2x \left[-\frac{1}{4g^2} F_{\mu\nu}^2 - \frac{\kappa}{4g^2} \epsilon^{\rho\mu\nu} A_\rho F_{\mu\nu} + \frac{\nu^2}{2} (D_\mu \vec{\phi})^2 - \frac{\lambda^2}{4} (D_\mu \vec{\phi} \times D_\nu \vec{\phi})^2 - V(\phi_n) \right], \quad (2)$$

where $D_\mu \vec{\phi}$ is the covariant derivative [29, 38]

$$D_\mu \vec{\phi} = \partial_\mu \vec{\phi} + A_\mu \vec{n} \times \vec{\phi}, \quad (3)$$

defining the coupling between the Abelian gauge field A_μ and the Skyrme field $\vec{\phi}$. The first contribution in Eq. (2) is the Maxwell term with $F_{\mu\nu} = \partial_\mu A_\nu - \partial_\nu A_\mu$ and A_μ being the $U(1)$ gauge field. The other contributions listed in order are: the Chern-Simons term, the nonlinear σ -model term, the Skyrme term, and the self-interacting potential. Besides, we have extracted a common energy factor E_0 [29, 41] setting the model energy scale which for our objectives we shall always consider $E_0 = 1$. Also, it will be assumed all the coupling constants are non-negative quantities. Moreover, the Chern-Simons coupling constant κ and the electromagnetic coupling g have mass dimension 1, the Skyrme coupling constant λ has mass dimension -1 , and ν is dimensionless.

We restrict our study of the model (2) to the case without the σ -model term ($\nu = 0$), thus, the starting point of our analysis will be the following Lagrangian density

$$\mathcal{L} = -\frac{1}{4g^2} F_{\mu\nu}^2 - \frac{\kappa}{4g^2} \epsilon^{\rho\mu\nu} A_\rho F_{\mu\nu} - \frac{\lambda^2}{4} (D_\mu \vec{\phi} \times D_\nu \vec{\phi})^2 - V, \quad (4)$$

it can be named the Maxwell-Chern-Simons restricted Skyrme model. The respective equation of motion of the gauge field reads

$$\partial_\sigma F^{\sigma\mu} - \frac{\kappa}{2} \epsilon^{\mu\alpha\beta} F_{\alpha\beta} = g^2 \vec{n} \cdot \vec{J}^\mu, \quad (5)$$

and the one for the Skyrme field results

$$D_\mu \vec{J}^\mu = -\frac{\partial V}{\partial \phi_n} \vec{n} \times \vec{\phi}. \quad (6)$$

The conserved current density $j^\mu = \vec{n} \cdot \vec{J}^\mu$ is defined in terms of the vector \vec{J}^μ given by

$$\vec{J}^\mu = \lambda^2 [\vec{\phi} \cdot (D^\mu \vec{\phi} \times D^\nu \vec{\phi})] (D_\nu \vec{\phi}). \quad (7)$$

Our effort will be focused to the study of stationary soliton solutions, this way, below we write the field equations ruling this regimen. Thus, from Eq. (5), the Gauss law reads,

$$\partial_i E_i - \kappa B = g^2 j_0, \quad (8)$$

with $j_0 = -\lambda^2 A_0 (\vec{n} \cdot \partial_i \vec{\phi})^2$, the electric charge density. We have defined the electric field components by $E_i = F_{0i} = -\partial_i A_0$ while the magnetic is given by $B = F_{12} = \epsilon_{ij} \partial_i A_j$. The Gauss law point out the mixing of the electric and magnetic sectors, an effect due to the presence of the Chern-Simons term. Clearly, Eq. (8) implies the field configurations besides to possess a nonzero magnetic flux Φ they also carry a nonzero total electric charge \mathcal{Q}_{em} . The relation between both physical quantities is obtained

by integrating (under appropriated boundary conditions) the Gauss law,

$$\mathcal{Q}_{\text{em}} = -\frac{\kappa}{g^2}\Phi, \quad (9)$$

where

$$\mathcal{Q}_{\text{em}} = \int d^2x j_0, \quad \Phi = \int d^2x B. \quad (10)$$

For the stationary Ampère law we get

$$\partial_i B - \kappa E_i + \lambda^2 g^2 (\vec{n} \cdot \partial_i \vec{\phi}) Q = 0. \quad (11)$$

Above, we have defined the quantity

$$Q \equiv \vec{\phi} \cdot (D_1 \vec{\phi} \times D_2 \vec{\phi}), \quad (12)$$

which also can be expressed by

$$Q = \vec{\phi} \cdot (\partial_1 \vec{\phi} \times \partial_2 \vec{\phi}) + \epsilon_{ij} A_i (\vec{n} \cdot \partial_j \vec{\phi}). \quad (13)$$

The first term $\vec{\phi} \cdot (\partial_1 \vec{\phi} \times \partial_2 \vec{\phi})$ is related to the topological charge or topological degree (also named winding number) of the Skyrme field [50],

$$\text{deg}[\vec{\phi}] = -\frac{1}{4\pi} \int d^2x \vec{\phi} \cdot (\partial_1 \vec{\phi} \times \partial_2 \vec{\phi}) = k, \quad (14)$$

being $k \in \mathbb{Z} \setminus 0$.

Similarly, the stationary equation of motion of the Skyrme field is given by

$$0 = \lambda^2 \epsilon_{ij} D_i (Q D_j \vec{\phi}) + \lambda^2 \partial_j [A_0^2 (\vec{n} \cdot \partial_j \vec{\phi})] (\vec{n} \times \vec{\phi}) + \frac{\partial V}{\partial \phi_n} (\vec{n} \times \vec{\phi}). \quad (15)$$

Until now all researches about solitons solutions obtained from the Lagrangian density (4) have not been able to engender self-dual or BPS configurations. Then, in order to obtain such a BPS structures we propose to next a modified version of the model (4) such that the gauge field equation remains unchanged.

III. SELF-DUAL MAXWELL-CHERN-SIMONS BABY SKYRME MODEL

The corresponding self-dual model is constructed by introducing a neutral scalar field which besides to interact only with the Skyrme field also modify the potential. Such a BPS Maxwell-Chern-Simons baby Skyrme model is described by the following Lagrangian density

$$\mathcal{L} = -\frac{1}{4g^2} F_{\mu\nu}^2 - \frac{\kappa}{4g^2} \epsilon^{\rho\mu\nu} A_\rho F_{\mu\nu} - \frac{\lambda^2}{4} (D_\mu \vec{\phi} \times D_\nu \vec{\phi})^2 + \frac{1}{2g^2} \partial_\mu \Psi \partial^\mu \Psi + \frac{\lambda^2}{2} (\vec{n} \cdot D_\mu \vec{\phi})^2 \Psi^2 - U, \quad (16)$$

where Ψ is the neutral scalar field, and U is the potential which now is a function of both the variable ϕ_n and the neutral scalar field, i.e., $U = U(\phi_n, \Psi)$. The procedure used to achieve the model (16) by means of the introduction of a neutral scalar field with the aim to attain a successful implementation of the Bogomol'nyi technique is already well known in literature. It was firstly used in the context of Maxwell-Chern-Simons-Higgs models [51]. Similar approaches in subsequent investigations have also successfully implemented as in [52, 53] and in some Lorentz-violating scenarios [54–57]. Further, it is important to mention the Lagrangian density (16) has a matching to a $\mathcal{N} = 2$ SUSY model, such a property can be verified in Ref. [48].

Furthermore, it is worthwhile to point out the penultimate term in (16) can be expressed as

$$(\vec{n} \cdot D_\mu \vec{\phi})^2 = (D_\mu \vec{\phi})^2 - (\vec{n} \times D_\mu \vec{\phi})^2, \quad (17)$$

which allows us to write the Lagrangian density at form

$$\mathcal{L} = -\frac{1}{4g^2} F_{\mu\nu}^2 - \frac{\kappa}{4g^2} \epsilon^{\rho\mu\nu} A_\rho F_{\mu\nu} - \frac{\lambda^2}{4} (D_\mu \vec{\phi} \times D_\nu \vec{\phi})^2 + \frac{1}{2g^2} \partial_\mu \Psi \partial^\mu \Psi + \frac{\lambda^2}{2} (D_\mu \vec{\phi})^2 \Psi^2 - \frac{\lambda^2}{2} (\vec{n} \times D_\mu \vec{\phi})^2 \Psi^2 - U. \quad (18)$$

In other words, the model given in (18) can be considered a type of generalized Maxwell-Chern-Simons-Skyrme model in (2+1) dimensions, including a σ -model like term, $(D_\mu \vec{\phi})^2 \Psi^2$, in which the function Ψ would play the role of the generalizing function.

As already mentioned, the gauge field equation corresponding to the model (16) is the same one of the model (4), i.e., the introduction of the neutral scalar field Ψ does not modify the gauge field equation which is given by Eq. (5). However, the Skyrme field equation of motion (6) suffers modification and now it reads

$$D_\mu \vec{J}^\mu = \left[-\lambda^2 \partial_\mu [(\vec{n} \cdot D^\mu \vec{\phi}) \Psi^2] - \frac{\partial U}{\partial \phi_n} \right] (\vec{n} \times \vec{\phi}). \quad (19)$$

The respective stationary version reads

$$\frac{\partial U}{\partial \phi_n} (\vec{n} \times \vec{\phi}) = \lambda^2 \partial_i [(\vec{n} \cdot \partial_i \vec{\phi}) (\Psi^2 - A_0^2)] (\vec{n} \times \vec{\phi}) - \lambda^2 \epsilon_{ij} D_i (Q D_j \vec{\phi}). \quad (20)$$

For last, the equation of motion of the neutral scalar field is

$$\partial_\mu \partial^\mu \Psi - \lambda^2 g^2 (\vec{n} \cdot D_\mu \vec{\phi})^2 \Psi + g^2 \frac{\partial U}{\partial \Psi} = 0. \quad (21)$$

In the next section, we will show how the BPS formalism is implemented. Along the procedure, the self-dual potential $U(\phi_n, \Psi)$ is determined allowing to obtain the energy lower bound and the self-dual equations satisfied by the solitonic configurations saturating such a bound.

A. The BPS structure

The stationary energy density of the model (16) is

$$\begin{aligned} \epsilon = & \frac{1}{2g^2}B^2 + \frac{1}{2g^2}(\partial_i A_0)^2 + \frac{\lambda^2}{2}(A_0)^2(\vec{n} \cdot \partial_i \vec{\phi})^2 + \frac{\lambda^2}{2}Q^2 \\ & + \frac{1}{2g^2}(\partial_i \Psi)^2 + \frac{\lambda^2}{2}\Psi^2(\vec{n} \cdot \partial_i \vec{\phi})^2 + U(\phi_n, \Psi), \end{aligned} \quad (22)$$

where we have used

$$Q^2 = \frac{1}{2}(D_i \vec{\phi} \times D_j \vec{\phi})^2. \quad (23)$$

Before we establish the field boundary conditions under the requiring for energy density be null when $|\vec{x}| \rightarrow \infty$, we set the vacuum condition for the Skyrme field

$$\lim_{|\vec{x}| \rightarrow \infty} \vec{\phi} = \hat{n}, \quad (24)$$

which provides

$$\lim_{|\vec{x}| \rightarrow \infty} \vec{n} \cdot \partial_i \vec{\phi} = 0, \text{ or } \lim_{|\vec{x}| \rightarrow \infty} \partial_i \vec{\phi} = \vec{0}. \quad (25)$$

The other boundary conditions arising from energy density (22) are

$$\lim_{|\vec{x}| \rightarrow \infty} B = 0, \quad \lim_{|\vec{x}| \rightarrow \infty} Q = 0, \quad (26)$$

$$\lim_{|\vec{x}| \rightarrow \infty} \partial_i A_0 = 0, \quad \lim_{|\vec{x}| \rightarrow \infty} \partial_i \Psi = 0, \quad (27)$$

$$\lim_{|\vec{x}| \rightarrow \infty} U(\phi_n, \Psi) = 0. \quad (28)$$

We still are able to set boundary conditions on the gauge field and the neutral scalar. Firstly, from (13) and $\lim_{|\vec{x}| \rightarrow \infty} Q = 0$, we conclude the potential vector satisfies

$$\lim_{|\vec{x}| \rightarrow \infty} A_i < \infty. \quad (29)$$

Secondly, from the energy density (22), the terms $(A_0)^2(\vec{n} \cdot \partial_i \vec{\phi})^2$ and $\Psi^2(\vec{n} \cdot \partial_i \vec{\phi})^2$ provide the fields A_0 and Ψ must remain finite when $|\vec{x}| \rightarrow \infty$.

The total energy is defined by integrating the energy density (22),

$$E = \int d^2x \epsilon. \quad (30)$$

Now, with the aim to implement the BPS formalism, we introduce two auxiliary functions, namely $\Sigma \equiv \Sigma(\phi_n, \Psi)$ and $Z \equiv Z(\phi_n)$ which we shall determine later. Thus, af-

ter some algebraic manipulations, the total energy reads

$$\begin{aligned} E = & \int d^2x \left[\frac{1}{2g^2} (B \pm \Sigma)^2 + \frac{\lambda^2}{2} (Q \mp Z)^2 \right. \\ & + \frac{1}{2g^2} (\partial_i A_0 \mp \partial_i \Psi)^2 + \frac{\lambda^2}{2} (A_0 \mp \Psi)^2 (\vec{n} \cdot \partial_i \vec{\phi})^2 \\ & \pm \lambda^2 A_0 \Psi (\vec{n} \cdot \partial_i \vec{\phi})^2 \mp \frac{1}{g^2} B \Sigma - \frac{1}{2g^2} \Sigma^2 \\ & \left. \pm \lambda^2 Q Z - \frac{\lambda^2}{2} Z^2 \pm \frac{1}{g^2} (\partial_i A_0) \partial_i \Psi + U \right]. \end{aligned} \quad (31)$$

By using the expression (13) and the Gauss law (8), we arrive at

$$\begin{aligned} E = & \int d^2x \left[\frac{1}{2g^2} (B \pm \Sigma)^2 + \frac{\lambda^2}{2} (Q \mp Z)^2 \right. \\ & + \frac{1}{2g^2} (\partial_i A_0 \mp \partial_i \Psi)^2 + \frac{\lambda^2}{2} (A_0 \mp \Psi)^2 (\vec{n} \cdot \partial_i \vec{\phi})^2 \\ & \pm \lambda^2 Z \vec{\phi} \cdot (\partial_1 \vec{\phi} \times \partial_2 \vec{\phi}) \pm \frac{1}{g^2} \partial_i (\Psi \partial_i A_0) \\ & \mp \frac{1}{g^2} \epsilon_{ji} (\partial_j A_i) (\Sigma - \kappa \Psi) \pm \lambda^2 \epsilon_{ij} A_i Z (\vec{n} \cdot \partial_j \vec{\phi}) \\ & \left. - \frac{1}{2g^2} \Sigma^2 - \frac{\lambda^2}{2} Z^2 + U \right]. \end{aligned} \quad (32)$$

where in the fourth row we have used $B = \epsilon_{ji} \partial_j A_i$.

At this point, we transform the fourth row of Eq. (32) in a total derivative. To achieve this, we set

$$\Sigma \equiv \lambda^2 g^2 W + \kappa \Psi, \quad (33)$$

being $W \equiv W(\phi_n)$ and, thus, the fourth row in (32) leads to

$$\pm \lambda^2 \epsilon_{ij} \left[(\partial_j A_i) W + A_i Z (\vec{n} \cdot \partial_j \vec{\phi}) \right]. \quad (34)$$

It becomes a total derivative by setting

$$\partial_j W = Z (\vec{n} \cdot \partial_j \vec{\phi}) \text{ such that } Z = \frac{\partial W}{\partial \phi_n}. \quad (35)$$

Therefore, the total energy becomes

$$\begin{aligned} E = & \int d^2x \left\{ \frac{1}{2g^2} \left[B \pm (\lambda^2 g^2 W + \kappa \Psi) \right]^2 \right. \\ & + \frac{\lambda^2}{2} \left[Q \mp \frac{\partial W}{\partial \phi_n} \right]^2 + \frac{\lambda^2}{2} (A_0 \mp \Psi)^2 (\vec{n} \cdot \partial_i \vec{\phi})^2 \\ & + \frac{1}{2g^2} (\partial_i A_0 \mp \partial_i \Psi)^2 \pm \lambda^2 \left(\frac{\partial W}{\partial \phi_n} \right) \vec{\phi} \cdot (\partial_1 \vec{\phi} \times \partial_2 \vec{\phi}) \\ & \pm \frac{1}{g^2} \partial_i (\Psi \partial_i A_0) \mp \lambda^2 \epsilon_{ij} \partial_j (A_i W) \\ & \left. - \frac{1}{2g^2} (\lambda^2 g^2 W + \kappa \Psi)^2 - \frac{\lambda^2}{2} \left(\frac{\partial W}{\partial \phi_n} \right)^2 + U \right\}, \end{aligned} \quad (36)$$

To continue with the implementation of the BPS formalism we require the potential $U(\phi_n, \Psi)$ be defined as

$$U(\phi_n, \Psi) = \frac{\lambda^2}{2} \left(\frac{\partial W}{\partial \phi_n} \right)^2 + \frac{\lambda^4 g^2}{2} \left(W + \frac{\kappa}{\lambda^2 g^2} \Psi \right)^2, \quad (37)$$

which is the one able to generate self-dual configurations. Notably, $W(\phi_n)$ plays the role of a ‘‘superpotential function’’, being its structure analogous the one we found in the literature, e.g., in the context of self-gravitating domain walls [58–60] or scalar field inflation [61–64] models. From henceforth, we shall call the function $W(\phi_n)$ as the superpotential.

The function $W(\phi_n)$ must be constructed (or proposed) such the self-dual potential $U(\phi_n, \Psi)$ satisfies the vacuum condition expressed in Eq. (28). Consequently, a brief analysis of the relation (37) allows us to impose the following boundary conditions for the superpotential

$$\lim_{\phi_n \rightarrow 1} W(\phi_n) = 0, \quad \lim_{\phi_n \rightarrow 1} \frac{\partial W}{\partial \phi_n} = 0, \quad (38)$$

and for the neutral scalar field,

$$\lim_{|\vec{x}| \rightarrow \infty} \Psi = 0. \quad (39)$$

Considering the boundary conditions (38) and (39), we observe the contributions of the total derivatives in the fourth row of Eq. (36) vanish, i.e.,

$$\int d^2x \epsilon_{ij} \partial_j (A_i W) = 0, \quad \int d^2x \partial_i (\Psi \partial_i A_0) = 0. \quad (40)$$

It is important to emphasize that the second expression in (40) also would be satisfied by the boundary condition on the electric field given in Eq. (27).

Therefore, we consider the total energy written as

$$E = \bar{E} + E_{\text{BPS}}, \quad (41)$$

where \bar{E} represents the integration composed by the quadratic terms,

$$\begin{aligned} \bar{E} = \int d^2x \left\{ \frac{1}{2g^2} \left[B \pm (\kappa \Psi + g^2 \lambda^2 W) \right]^2 \right. \\ \left. + \frac{\lambda^2}{2} \left[Q \mp \frac{\partial W}{\partial \phi_n} \right]^2 + \frac{1}{2g^2} (\partial_i A_0 \mp \partial_i \Psi)^2 \right. \\ \left. + \frac{\lambda^2}{2} (A_0 \mp \Psi)^2 (\vec{n} \cdot \partial_i \vec{\phi})^2 \right\}, \quad (42) \end{aligned}$$

and E_{BPS} defines the energy lower bound,

$$E_{\text{BPS}} = \pm \lambda^2 \int d^2x \left(\frac{\partial W}{\partial \phi_n} \right) \vec{\phi} \cdot (\partial_1 \vec{\phi} \times \partial_2 \vec{\phi}). \quad (43)$$

The total energy (41) satisfy the inequality

$$E \geq E_{\text{BPS}}, \quad (44)$$

because $\bar{E} \geq 0$. Then, the energy lower bound will be achieved when the fields possess configurations such that $\bar{E} = 0$, i.e., the field configurations be solutions of the following set of first-order differential equations:

$$B = \mp g^2 \lambda^2 W \mp \kappa \Psi, \quad (45)$$

$$Q = \pm \frac{\partial W}{\partial \phi_n}, \quad (46)$$

$$\partial_i \Psi = \pm \partial_i A_0, \quad \Psi = \pm A_0. \quad (47)$$

They are the so-called self-dual or BPS equations corresponding to the model (16). This set of equations possess a correspondence [65, 66] with the BPS equations of an extended supersymmetric model. Indeed, the model (16) is related to the bosonic part of a $\mathcal{N} = 2$ SUSY extension [48], so that the solutions of the BPS equations are classified as being of the type 1/4-BPS associated to the existence of a nontrivial phase of the SUSY extended model.

From (47), we observe that $\Psi = \pm A_0$ automatically satisfies both equations, consequently, the self-dual or BPS charged solitons are described by the equations

$$B = \mp g^2 \lambda^2 W - \kappa A_0, \quad (48)$$

$$Q = \pm \frac{\partial W}{\partial \phi_n}, \quad (49)$$

together with the Gauss law (8),

$$\partial_i \partial_i A_0 + \kappa B = g^2 \lambda^2 A_0 (\vec{n} \cdot \partial_i \vec{\phi})^2. \quad (50)$$

In addition, the boundary condition (39) in the BPS limit implies the scalar potential must satisfy

$$\lim_{|\vec{x}| \rightarrow \infty} A_0 = 0. \quad (51)$$

B. Equivalence between the BPS and Euler-Lagrange equations

In this section let us to show that from the BPS equations we recover the stationary Euler-Lagrange equations provided by the Lagrangian density (16), namely, the Ampère law (11) and the Skyrme field equation (20).

1. Recovering the Ampère law

First, we take the partial derivative of the BPS equation (48) getting

$$\partial_i B = \mp g^2 \lambda^2 \frac{\partial W}{\partial \phi_n} \partial_i \phi_n \mp \kappa \partial_i \Psi, \quad (52)$$

and now by using the BPS equations (49) and (47) we obtain

$$\partial_i B = -g^2 \lambda^2 Q \partial_i \phi_n - \kappa \partial_i A_0, \quad (53)$$

being exactly the stationary Ampère law.

2. Recovering the Skyrme field equation

With the aim to recover the stationary field equation (20) for the Skyrme field we begin rewriting the BPS equation (49) as

$$Q(D_j \vec{\phi}) = \pm \frac{\partial W}{\partial \phi_n} (D_j \vec{\phi}), \quad (54)$$

and applying the quantity $\lambda^2 \epsilon_{ij} D_i$ in both sides results

$$\begin{aligned} \lambda^2 \epsilon_{ij} D_i (Q D_j \vec{\phi}) &= \pm \lambda^2 \epsilon_{ij} D_i \left(\frac{\partial W}{\partial \phi_n} D_j \vec{\phi} \right) \\ &= \pm \lambda^2 \epsilon_{ij} \frac{\partial^2 W}{\partial \phi_n^2} (\partial_i \phi_n) D_j \vec{\phi} \\ &\quad \pm \frac{\lambda^2}{2} \frac{\partial W}{\partial \phi_n} \epsilon_{ij} [D_i, D_j] \vec{\phi}. \end{aligned} \quad (55)$$

Now, we use the following identities

$$\epsilon_{ij} (\partial_i \phi_n) D_j \vec{\phi} = -Q(\vec{n} \times \vec{\phi}), \quad (56)$$

$$\epsilon_{ij} [D_i, D_j] \vec{\phi} = 2B(\vec{n} \times \vec{\phi}), \quad (57)$$

to arrive at

$$\begin{aligned} \lambda^2 \epsilon_{ij} D_i (Q D_j \vec{\phi}) &= \mp \lambda^2 \frac{\partial^2 W}{\partial \phi_n^2} Q(\vec{n} \times \vec{\phi}) \\ &\quad \pm \lambda^2 \frac{\partial W}{\partial \phi_n} B(\vec{n} \times \vec{\phi}). \end{aligned} \quad (58)$$

Inserting the BPS equations (48) and (49), just in the right side, we obtain

$$\begin{aligned} \lambda^2 \epsilon_{ij} D_i (Q D_j \vec{\phi}) &= -\lambda^2 \frac{\partial^2 W}{\partial \phi_n^2} \frac{\partial W}{\partial \phi_n} (\vec{n} \times \vec{\phi}) \\ &\quad - \lambda^2 \frac{\partial W}{\partial \phi_n} (g^2 \lambda^2 W + \kappa \Psi) (\vec{n} \times \vec{\phi}). \end{aligned} \quad (59)$$

The right-hand can be write in terms of the derivative of the potential (37) with respect to ϕ_n , thus,

$$\lambda^2 \epsilon_{ij} D_i (Q D_j \vec{\phi}) = -\frac{\partial U}{\partial \phi_n} (\vec{n} \times \vec{\phi}). \quad (60)$$

It is the Skyrme field equation (20) in Bogomol'nyi limit. Therefore, we have verified that the BPS equations imply in both stationary field equations, Ampère law and the Skyrme field equation.

IV. ROTATIONALLY SYMMETRIC SKYRMIONS

We investigate solitons rotationally symmetric saturating the energy lower bound (43). Henceforth, without

loss of generality, we set $\vec{n} = (0, 0, 1)$ such that $\phi_n = \phi_3$ and set the usual *ansatz* for the Skyrme field [29],

$$\vec{\phi}(r, \theta) = \begin{pmatrix} \sin f(r) \cos N\theta \\ \sin f(r) \sin N\theta \\ \cos f(r) \end{pmatrix}, \quad (61)$$

where r and θ are polar coordinates, $N = \text{deg}[\vec{\phi}]$ is the winding number introduced in (14) and $f(r)$ a regular function satisfying boundary conditions

$$f(0) = \pi, \quad \lim_{r \rightarrow \infty} f(r) = 0. \quad (62)$$

The representation (61) is a two-dimensional version of the hedgehog ansatz used in the three-dimensional Skyrme model [67].

For the gauge field A_μ , we consider the ansatz

$$A_i = -\epsilon_{ij} x_j \frac{Na(r)}{r^2}, \quad A_0 = \omega(r), \quad (63)$$

where the profile functions $a(r)$ and $\omega(r)$ are well behaved functions satisfying the boundary conditions,

$$a(0) = 0, \quad \lim_{r \rightarrow \infty} a(r) = a_\infty, \quad (64)$$

$$\omega(0) = \omega_0, \quad \lim_{r \rightarrow \infty} \omega(r) = 0, \quad \lim_{r \rightarrow \infty} \frac{d\omega}{dr} = 0, \quad (65)$$

where a_∞ and ω_0 are finite constants.

By convenience, we now introduce the field redefinition [41] as follows:

$$\phi_3 = \cos f \equiv 1 - 2h, \quad (66)$$

with the field $h = h(r)$ obeying

$$h(0) = 1, \quad \lim_{r \rightarrow \infty} h(r) = 0. \quad (67)$$

The boundary conditions for the superpotential $W(h)$ are

$$\lim_{r \rightarrow 0} W(h) = W_0, \quad \lim_{r \rightarrow \infty} W(h) = 0, \quad \lim_{r \rightarrow \infty} \frac{dW}{dh} = 0, \quad (68)$$

where W_0 is a positive finite constant and the two last conditions are consequence of Eq. (38).

The magnetic field and the electric field result be

$$B = \frac{N da}{r dr}, \quad E_r = -\frac{d\omega}{dr}. \quad (69)$$

whereas the energy lower bound (43) or BPS bound becomes

$$E \geq E_{\text{BPS}} = \pm 2\pi \lambda^2 N W_0. \quad (70)$$

where W_0 is a constant defined in Eq. (68).

Under the ansatz, the BPS equations become

$$\frac{N da}{r dr} + \lambda^2 g^2 W + \kappa \omega = 0, \quad (71)$$

$$\frac{4N}{r}(1+a)\frac{dh}{dr} + \frac{dW}{dh} = 0, \quad (72)$$

while the Gauss law (50) gives

$$\frac{d^2\omega}{dr^2} + \frac{1}{r}\frac{d\omega}{dr} + \frac{\kappa N}{r}\frac{da}{dr} = 4\lambda^2 g^2 \omega \left(\frac{dh}{dr}\right)^2. \quad (73)$$

Note that in the BPS equations (71) and (72), without a loss of generality, we have chosen the upper sign. Such a assumption will be considered in the remaining of the manuscript.

Similarly, we write the self-dual potential

$$U(h, \omega) = \frac{\lambda^2}{8} \left(\frac{dW}{dh}\right)^2 + \frac{\lambda^4 g^2}{2} \left(W + \frac{\kappa}{\lambda^2 g^2} \omega\right)^2, \quad (74)$$

and by using the BPS equation the energy density becomes

$$\epsilon_{\text{BPS}} = \frac{B^2}{g^2} + \frac{1}{g^2} \left(\frac{d\omega}{dr}\right)^2 + 4\lambda^2 \omega^2 \left(\frac{dh}{dr}\right)^2 + \frac{\lambda^2}{4} \left(\frac{dW}{dh}\right)^2, \quad (75)$$

we call it the BPS energy density.

In the next subsections we study the behavior at origin and when $r \rightarrow \infty$ of the self-dual profiles by solving the BPS equations (71), (72) and the Gauss law (73).

A. Behavior of the profiles at origin

We perform the analysis around the origin ($r = 0$) by considering the following boundary conditions

$$h(0) = 1, \quad a(0) = 0, \quad \omega(0) = \omega_0, \quad \lim_{r \rightarrow 0} W(h) = W_0, \quad (76)$$

where the superpotential $W(h)$ is considered to be a well-behaved function with W_0 being a positive finite quantity. Hence, we find the following behavior for the field profiles:

$$h(r) \approx 1 - \frac{(W_h)_{h=0}}{8N} r^2 + \frac{(W_h)_{h=0} (W_{hh})_{h=0}}{128N^2} r^4, \quad (77)$$

$$a(r) \approx -C_0 r^2 + \frac{g^2 \lambda^2 (W_h)_{h=0}^2 - 4\kappa^2 N^2 C_0}{32N^2} r^4, \quad (78)$$

$$\begin{aligned} \omega(r) \approx \omega_0 + \frac{\kappa N C_0}{2} r^2 \\ - \frac{\kappa g^2 \lambda^2 (W_h)_{h=0}^2 - 4\kappa^3 N^2 C_0}{128N} r^4, \end{aligned} \quad (79)$$

where $W_h = dW/dh$, $W_{hh} = d^2W/dh^2$, and we have defined the constant

$$C_0 = \frac{g^2 \lambda^2 W_0 + \kappa \omega_0}{2N}. \quad (80)$$

The behavior for magnetic and electric field near to

the origin are

$$B(r) \approx -2NC_0 + \frac{g^2 \lambda^2 (W_h)_{h=0}^2 - 4N^2 \kappa^2 C_0}{8N} r^2, \quad (81)$$

$$E_r(r) \approx -\kappa N C_0 r + \frac{\kappa g^2 \lambda^2 (W_h)_{h=0}^2 - 4\kappa^3 N^2 C_0}{32N} r^3, \quad (82)$$

respectively, while the BPS energy density gives

$$\begin{aligned} \epsilon_{\text{BPS}} \approx \frac{4N^2 C_0^2}{g^2} + \frac{\lambda^2}{4} (W_h)_{h=0} + \left[\frac{3\kappa^2 N^2 C_0^2}{g^2} \right. \\ \left. + \frac{\lambda^2 \omega_0^2 (W_h)_{h=0}^2}{4N^2} - \frac{\lambda^2 C_0 (W_h)_{h=0}^2}{2} \right. \\ \left. - \frac{1}{16} \frac{\lambda^2 (W_h)_{h=0}^2 (W_{hh})_{h=0}}{N} \right] r^2. \end{aligned} \quad (83)$$

It is verified that the amplitude of the BPS energy density at the origin increase in accordance with the growth of the electromagnetic coupling g .

B. Behavior of the profiles for large values of r

The behavior of the fields when $r \rightarrow \infty$ is performed by taking the following boundary conditions,

$$h(\infty) = 0, \quad a(\infty) = a_\infty, \quad \omega(\infty) = 0, \quad \lim_{r \rightarrow \infty} W(h) = 0. \quad (84)$$

Besides that, we consider a superpotential $W(h)$ behaving as

$$W(h) \approx \frac{h^\sigma}{\lambda^2}, \quad (85)$$

with the parameter $\sigma \geq 2$. Under the boundary conditions (84), the asymptotic analysis leads us to two type of Skyrme field profiles: (i) for $\sigma = 2$ we have found soliton solutions whose tail decays following an exponential-law type $e^{-\alpha r^2}$ ($\alpha > 0$); (ii) for $\sigma > 2$ the profiles of the Skyrme field have a power-law decay $r^{-\beta}$ ($\beta > 0$). At same time, for $\sigma \geq 2$ the gauge field profiles $a(r)$ and $\omega(r)$ decay following an exponential-law type e^{-mr} ($m > 0$).

1. Behavior of the profiles for $\sigma = 2$

We take a superpotential whose behavior is

$$W(h) \approx \frac{h^2}{\lambda^2}, \quad (86)$$

such that the field profiles possess the following asymptotic behavior

$$h(r) \approx C_\infty^{(h)} e^{-\Lambda r^2}, \quad (87)$$

$$a(r) \approx a_\infty - C_\infty \sqrt{r} e^{-\kappa r}, \quad (88)$$

$$\omega(r) \approx -C_\infty \frac{N}{\sqrt{r}} e^{-\kappa r}, \quad (89)$$

where $C_\infty^{(h)}$ and C_∞ are arbitrary constants and the quantity Λ has been defined as

$$\Lambda = \frac{1}{4N\lambda^2(1+a_\infty)}. \quad (90)$$

In addition, the magnetic and electric fields for large values of r behave as

$$B(r) \approx C_\infty \frac{N\kappa}{\sqrt{r}} e^{-\kappa r}, \quad (91)$$

$$E_r(r) \approx -C_\infty \frac{N\kappa}{\sqrt{r}} e^{-\kappa r}, \quad (92)$$

respectively. We must highlight the gauge field behavior (including the electric and magnetic fields) resembles the one of the Abrikosov-Nielsen-Olesen vortices arising in Abelian Higgs models [68–70]. Remembering the Maxwell-Higgs electrodynamics is the relativistic counterpart of the Ginzburg-Landau theory of superconductivity and, the BPS limit separates the phases describing the Type-I and Type-II superconductivity. Furthermore, the behavior shows explicitly the Chern-Simons coupling constant κ plays the role of the effective mass of the gauge field.

2. Behavior of the profiles for $\sigma > 2$

In this case, we consider a superpotential that obeys

$$W(h) \approx \frac{h^\sigma}{\lambda^2}. \quad (93)$$

Hence, when $r \rightarrow \infty$, the field profiles have the following asymptotic behavior:

$$h(r) \approx \left(\frac{C_\infty^{(h)}}{r^2} \right)^{1/(\sigma-2)}, \quad (94)$$

$$a(r) \approx a_\infty - C_\infty \sqrt{r} e^{-\kappa r}, \quad (95)$$

$$\omega(r) \approx -C_\infty \frac{N}{\sqrt{r}} e^{-\kappa r}, \quad (96)$$

where C_∞ is an arbitrary constant and $C_\infty^{(h)}$ defined as

$$C_\infty^{(h)} = \frac{8N\lambda^2(a_\infty + 1)}{\sigma(\sigma - 2)}. \quad (97)$$

We note the profiles of the Skyrme field follow a power-law decay contrasting the behavior for $\sigma = 2$ given in Eq. (87). Field profiles following a power-law decay for large distances are named *delocalized*. This type of solutions have appeared in the study of two-component superconductors [72], diamagnetic vortices [74] and in some k -generalized Abelian Higgs models [75]. On the other hand, the gauge field profiles $a(r)$ and $\omega(r)$ remain localized because they follow the same behavior of the ones analyzed in the previous case $\sigma = 2$ and, consequently, the magnetic and electric field behaviors are given by Eqs. (91) and (92), respectively.

V. NUMERICAL SOLUTIONS

A. Numerical solutions for $\sigma = 2$

Our first numerical analysis is devoted to solve the BPS equations (71), (72) and the Gauss law (73) by considering the superpotential

$$W(h) = \frac{h^2}{\lambda^2}. \quad (98)$$

Further, we set $N = 1$, $\lambda = 1$, $\kappa = 1$, and running the electromagnetic coupling constant g . The resulting solutions are shown in Figs. 1-6.

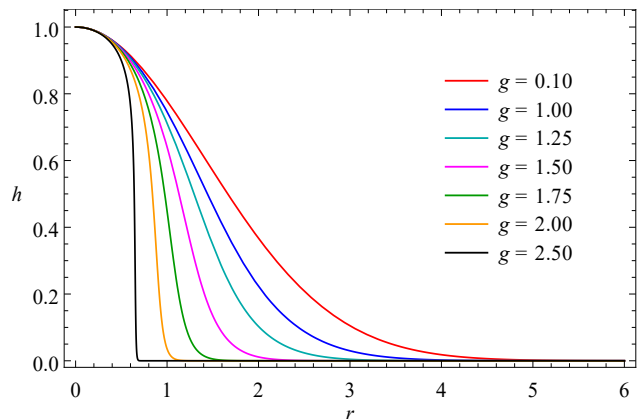


FIG. 1. Skyrme field profiles $h(r)$.

The profile functions $h(r)$ characterizing the Skyrme field are plotted in Fig. 1. Note that for increasing values of g the profiles become more localized around the origin. Also, for sufficiently large values of g (in our analysis, $g \gtrsim 2.5$), the profiles rapidly attain the vacuum value acquiring a structure seeming the one of a compacton (soliton of finite extent having its exact vacuum value outside of the compact region [71]). The arising of the compactonlike structure is consistent with the behavior (87) of the Skyrme field profile which yielding a fast exponential decay in the strong coupling limit of g ,

i.e., the parameter $\Lambda \rightarrow \infty$ as a consequence of $a_\infty \rightarrow -1$ (see Fig. 2).

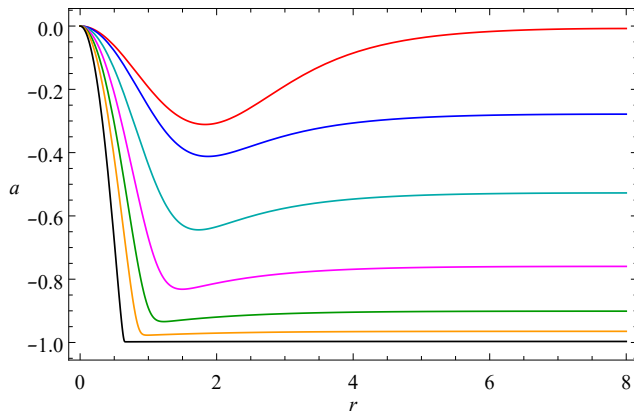


FIG. 2. Vector potential profiles $a(r)$. The profile for $g = 0.1$ (red line) has been rescaled by multiplying by 100. Conventions as in Fig. 1.

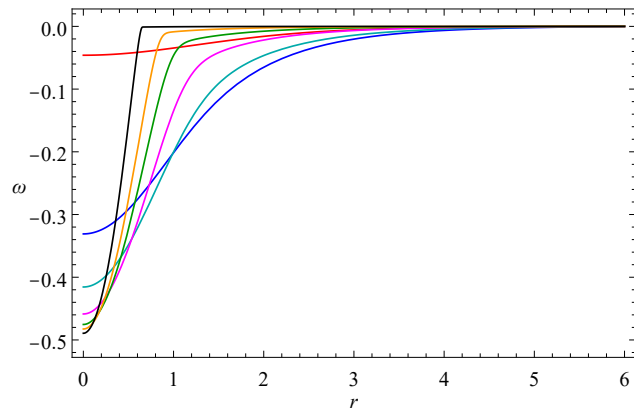


FIG. 3. Scalar potential $\omega(r)$. The profile for $g = 0.1$ (red line) has been rescaled by multiplying by 10. Conventions as in Fig. 1.

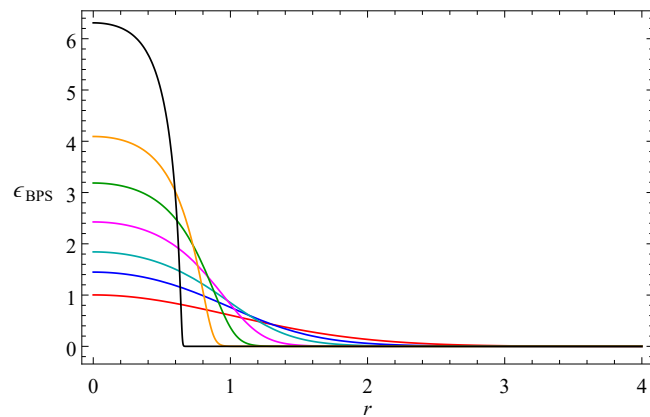


FIG. 4. BPS energy density $\epsilon_{\text{BPS}}(r)$. Conventions as in Fig. 1.

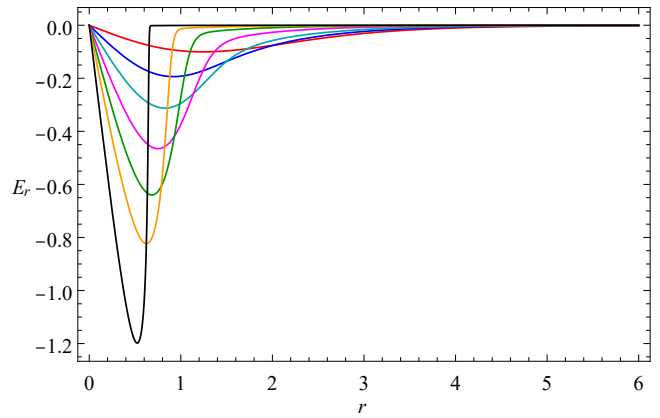


FIG. 5. Electric field $E_r(r)$. The profile for $g = 0.1$ (black dotted line) has been rescaled by multiplying by 50. Conventions as in Fig. 1.

Figure 2 depicts the vector potential profiles $a(r)$. Unlike of the case of the uncharged BPS solitons solutions approached in [41], here the vector potential profiles present an inverted ringlike shape (in our analysis such a feature is better seen in the interval $0 < g < 2$) which goes vanishing for sufficiently large values of g when the vector potential achieves a constant vacuum value $a_\infty \rightarrow -1$. As previously commented, when the vacuum value $a_\infty \rightarrow -1$ the format of the soliton profiles become compactonlike structures. It is worth emphasize that the arising of ringlike structures is associated to the presence of Chern-Simons term. In order to better visualize the ringlike effect for weak coupling, the profile for $g = 0.1$ (red line) was rescaled by multiplying it by 100.

The profiles for the scalar potential $\omega(r)$ and BPS energy density $\epsilon_{\text{BPS}}(r)$ are shown in Figs. 3 and 4, respectively. In both cases the amplitude at origin (in absolute value) increases with the growing of g . It is again observed the profiles for sufficiently large values of g present the compactonlike format.

The profiles of the electric field $E_r(r)$ are present in Fig. 5. The profiles are rings whose maximum amplitude is localized closer to the origin as the coupling constant g grows besides, they gain the compactonlike form. Furthermore, we have done a rescaling (multiplying by 50) the profile for $g = 0.1$ (red line) in order to the ring format becomes more visible. The numerical solutions tell us the electric field is negative for all values of r and g .

Figure 6 depicts the profiles of the magnetic field $B(r)$ for a set of values of the coupling constant g . At first sight, we observe whenever g increases, the absolute value of the amplitude in $r = 0$ also increases besides the profiles become more localized around the origin acquiring a compactonlike format. However, for sufficiently large values of r , a close zoom on the profiles (see insertion in Fig. 6) reveals a flipping (signal inversion) of the magnetic field which directly implies in a localized magnetic flux inversion. Such a flipping of the magnetic field becomes clearer by seeing Eqs. (91) and (92) given the behavior of

the magnetic and electric fields, they telling us that for large values of r the fields have opposite signals. Thus, being the electric field always negative, for large distances the magnetic field will be positive. In our analysis the maximum amplitude of the inversion grows in the interval of $0 < g \leq 1.2$, thereafter, decreases continuously for $g > 1.2$ until it disappears for sufficiently large values of the coupling constant g . We can highlight such a localized magnetic flux inversion in the present BPS model is a genuine effect due to presence of the Maxwell-Chern-Simons term, once that such a effect is absent in others gauged BPS baby Skyrme models in which the Maxwell's contribution [41] or the Chern-Simons contribution [33] have been analyzed individually.

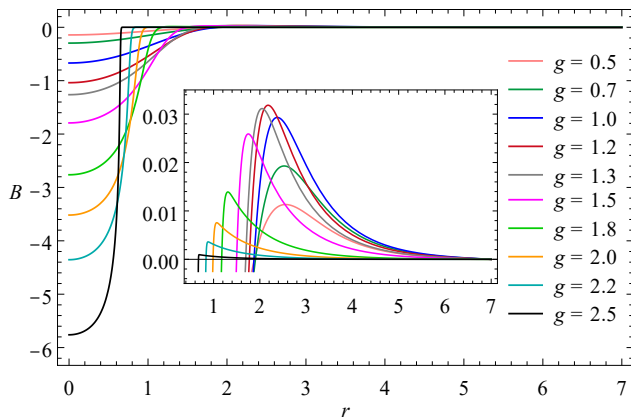


FIG. 6. Magnetic field $B(r)$.

The flipping of the magnetic field is a peculiar phenomenon which also has been reported on some other $(2+1)$ -dimensional systems. For example, such a behavior arises in the study of two-component superconductors whose fractional vortices present a delocalized magnetic field [72]. It also occurs in some Lorentz-violating Maxwell-Higgs electrodynamics [54, 55, 73] or in the context of Lorentz-violating gauged $O(3)$ σ -model [56].

B. Numerical solutions for $\sigma > 2$

Our second numerical analysis is performed by considering the superpotential

$$W(h) = \frac{h^\sigma}{\lambda^2}, \quad (99)$$

to solve the set of equations (71), (72), (73) for different values of the parameter σ and fixing $N = 1$, $\lambda = 1$, $\kappa = 1$, $g = 1$. The numerical profiles are shown in Figs. 7-12.

Figure 7 shows clearly that for $\sigma > 2$ the Skyrme field profile $h(r)$ decay more slowly to its vacuum value whenever σ increases, in according with the power-law given in Eq. (94).

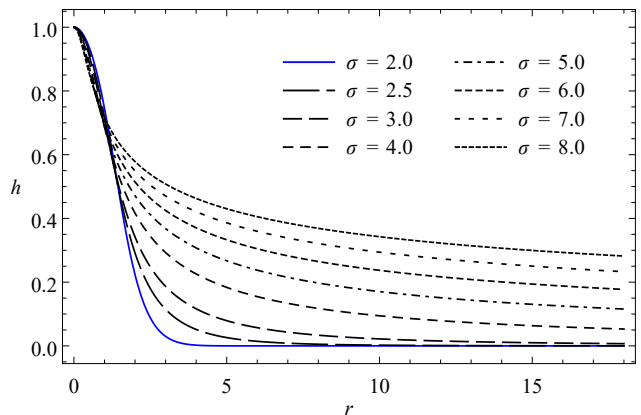


FIG. 7. Skyrme field profiles $h(r)$ for different values of σ in superpotential (99).

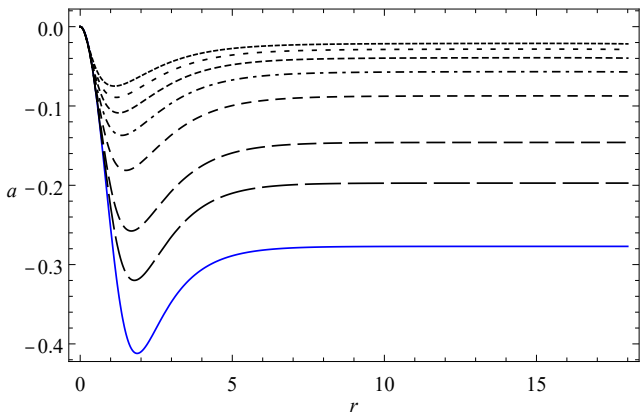


FIG. 8. Vector potential profiles $a(r)$. Conventions as in Fig.7.

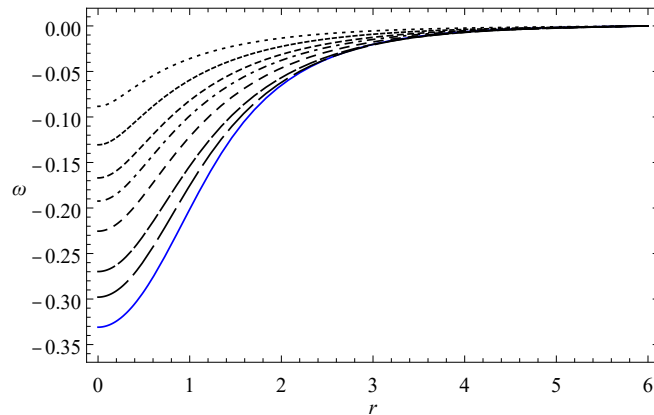
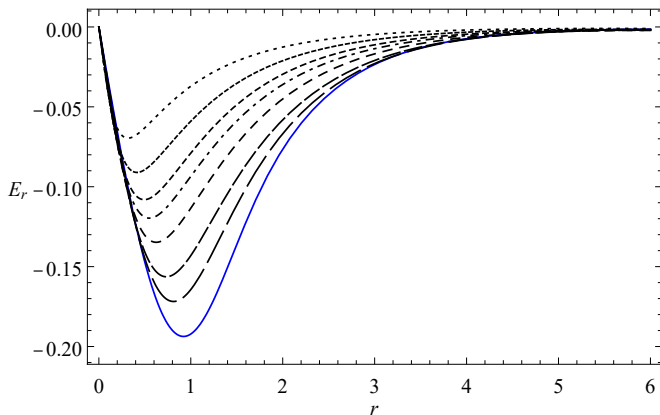
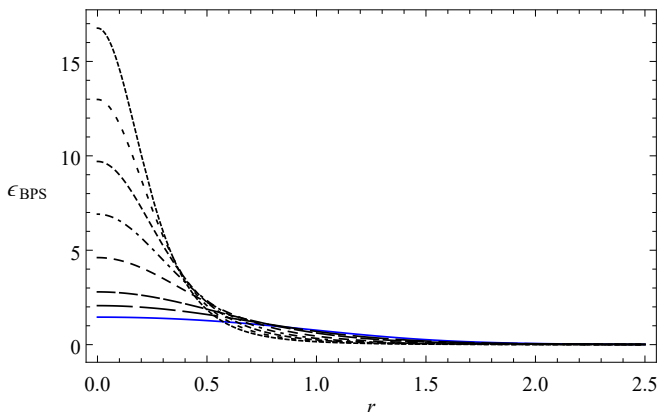


FIG. 9. Scalar potential $\omega(r)$. Conventions as in Fig. 7.

The general characteristics for profiles of the vector potential $a(r)$, scalar potential $\omega(r)$, electric field $E_r(r)$, self-dual energy density $\epsilon_{\text{BPS}}(r)$ and magnetic field $B(r)$ are similar to the ones already described in previous subsection, but becomes more and more localized near to at

FIG. 10. Electric field $E_r(r)$. Conventions as in Fig. 7.FIG. 11. BPS density energy $\epsilon_{\text{BPS}}(r)$. Conventions as in Fig. 7.

origin with the growth of the parameter σ , see Figs. 8-12. Nevertheless, it is worthwhile some comments about the vector potential and magnetic field. In Fig. 8, we note the ringlike structures of the vector potential profiles are vanishing as increasing of σ whereas $a(r)$ tends to zero. As consequence of such a behavior, the flip of the magnetic field also is present and its maximum amplitude diminishes with the increasing of the σ , see Fig. 12.

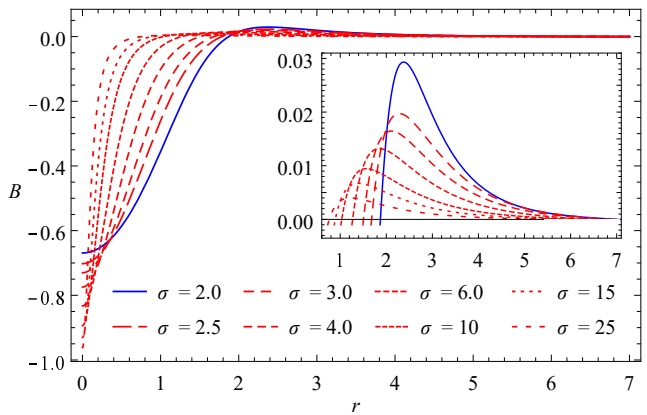
C. Magnetic flux and electric charge

The numerical results presented in the cases of $\sigma = 2$ allow us to analyze important results about the magnetic flux and the total electric charge.

The total magnetic flux is

$$\Phi = 2\pi \int_0^\infty r dr B \equiv 2\pi N a_\infty, \quad (100)$$

where we have considered the boundary conditions established in Eq. (64), because of the boundary condition (29) the parameter a_∞ is a finite real constant. There-

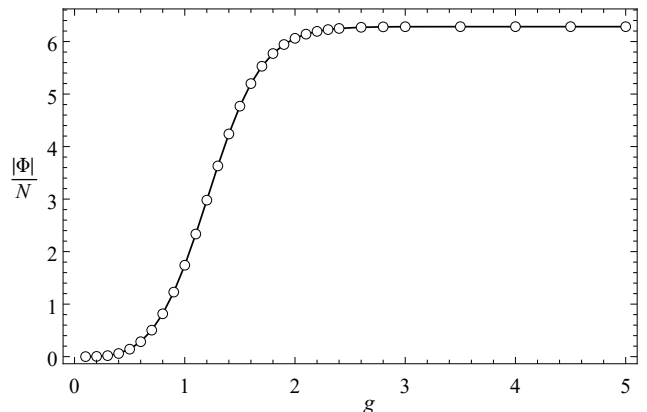
FIG. 12. Magnetic field $B(r)$ for other values of σ in superpotential (99).

fore, the magnetic flux is in general a nonquantized quantity (in the topological sense), unlike the one belonging to the Chern-Simons Abelian Higgs models [76, 77]. However, recent investigations have been shown it is possible to obtain quantized magnetic flux in some Skyrme models [31, 32, 78].

From expression (9), the total electric charge yields

$$Q_{\text{em}} = -\frac{2\pi\kappa N}{g^2} a_\infty, \quad (101)$$

showing it is nonquantized, too.

FIG. 13. The magnetic flux $|\Phi|$ in units of N as a function of the gauge coupling g for the superpotential (98), fixing $\lambda = 1$ and $\kappa = 1$.

We observe in the description of the Fig. 2 that for a sufficiently strong coupling g the vacuum value of the potential vector $a_\infty \rightarrow -1$, thus, the magnetic flux (100) becomes quantized in this limit, such as it is shown in Fig. 13. This effective quantization implies that the total electric charge (101) also becomes quantized in such regime.

Figure 14 we depict the behavior of the total electric charge as a function of the coupling constants g [$Q_{\text{em}}(g)$]

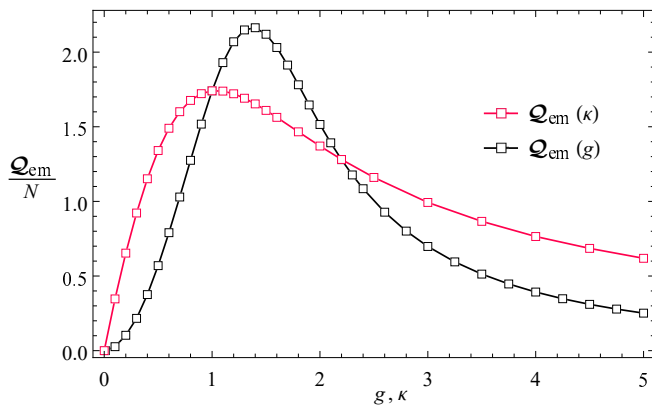


FIG. 14. The total electric charge in units of N as a function of both the constant electromagnetic coupling $\mathcal{Q}_{\text{em}}(g)$ and Chern-Simons coupling $\mathcal{Q}_{\text{em}}(\kappa)$ for the superpotential (98) with $\lambda = 1$.

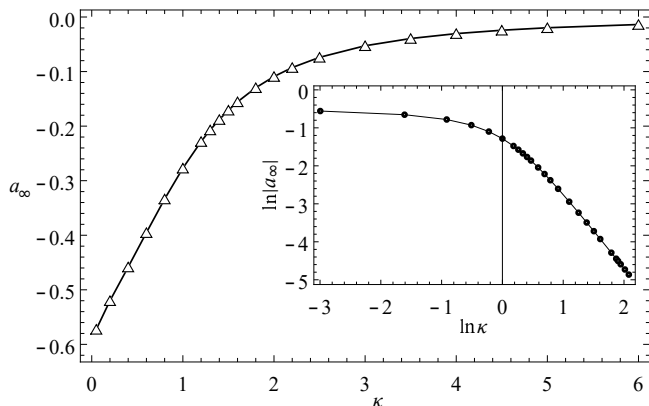


FIG. 15. The gauge vacuum value a_∞ as a function of the Chern-Simons coupling κ by assuming the superpotential (98) with $g = 1$, $\lambda = 1$ and $N = 1$. The insertion shows the logarithm of the absolute value of a_∞ as function of the logarithm of κ .

with κ fixed] and κ [$\mathcal{Q}_{\text{em}}(\kappa)$ with g fixed] by adopting the superpotential (98) with $\lambda = 1$. For the first analysis, it is fixed $\kappa = 1$ (black line-squared), we note the total electric charge $\mathcal{Q}_{\text{em}}(g)$ increases in accordance with g until it attains its maximum value at $g_{\text{max}} \simeq 1.387$, after the electric charge diminishes when g increases continuously, i.e., $\mathcal{Q}_{\text{em}}(g) \sim g^{-2}$ for $g \gg g_{\text{max}}$, compatible with Eq. (101).

The second analysis presented in Fig. 14 is performed by considering the gauge coupling constant fixed, $g = 1$ (red line-squared). We observe the the total electric charge $\mathcal{Q}_{\text{em}}(\kappa)$ grows as κ and reaches its maximum value at $\kappa_{\text{max}} \simeq 1.045$, from then on, gradually lessens with the continuous growth of the Chern-Simons coupling. Although that behavior is not directly explained by Eq. (101), we find numerically that for the interval $0 < \kappa < \kappa_{\text{max}}$ the vacuum value a_∞ seems to grow linearly with κ , see Fig. 15. Already for $\kappa > \kappa_{\text{max}}$, the values of a_∞ increase slower than growth of coupling κ ;

this behavior can be better understood by analyzing the insertion into Fig. 15, where we have $\ln|a_\infty|$ as function of $\ln\kappa$: we note that $|a_\infty| \sim \kappa^{-2}$ for $\kappa \gg \kappa_{\text{max}}$. Such an offbeat behavior is similar to the one of topological vortices obtained in the Chern-Simons $O(3)$ σ -model discussed in [79].

Now let us briefly comment about the magnetic flux and total electric charge for the case $\sigma > 2$. In Fig. 8, we note that for a fixed value of the gauge coupling g , the vacuum value a_∞ goes to zero continuously as σ grows, i.e., $\lim_{\sigma \rightarrow \infty} a_\infty = 0$. Consequently, the magnetic flux and the total electric charge become null. An analogous result was obtained in the generalized Chern-Simons baby Skyrme model [33].

VI. CONCLUSIONS AND REMARKS

We have shown the existence of BPS charged configurations in a gauged baby Skyrme model (16) whose gauge field is governed by the Maxwell-Chern-Simons action. The BPS model (16) is constructed by introducing a scalar field Ψ into the model (2) which couples adequately to the Skyrme field $\vec{\phi}$ but it does not couples to the gauge field. The successful implementation of the BPS technique allows to obtain the energy lower bound (is related to the topological charge of the Skyrme field) and hence the self-dual or BPS equations whose solutions saturate this bound. We point out the introduction of a superpotential function determining the self-dual potential is the important step in the successful implementation of the BPS technique. Such a superpotential is considered to be a well-behaved function in the whole target space and plays the important role by defining the BPS configurations. It is worth mentioning the model (16) has a correspondence with a $\mathcal{N} = 2$ SUSY extension model possessing self-dual or BPS structure. Besides, the solutions of the Eqs. (48) and (49) correspond to the type 1/4-BPS related to the nontrivial phase of the supersymmetric model [48].

With the aim to study the properties of the BPS configurations we have used a rotationally symmetric ansatz. In such ansatz it is verified the total energy (70) of the self-dual configurations is proportional to the topological charge N of the Skyrme field, thus, it is quantized. Then, we analyze the asymptotic behavior ($r \rightarrow \infty$) of the solutions by choosing a superpotential function that in such a limit behaves as $W(h) \approx h^\sigma/\lambda^2$. It has allowed to found two classes of self-dual profiles for the Skyrme field: the first class was obtained by considering $\sigma = 2$ which provides solutions whose tail decays following an exponential-law $e^{-\Lambda r^2}$ with Λ given in Eq. (90). The second class occurs for $\sigma > 2$, they are solutions whose tail decays following a power-law $r^{-\beta(\sigma)}$, with $\beta(\sigma) = 2/(\sigma - 2)$, see Eq. (94). For both classes of Skyrme profiles, the respective gauge fields possess an exponential-law type $e^{-\kappa r}$ (i.e., the Chern-Simons cou-

pling constant becomes the gauge field mass) very similar to behavior found for such fields in Abelian Higgs models describing Abrikosov-Nielsen-Olesen vortices.

Next, we dedicate our effort to solve numerically the differential equations describing the BPS configurations in order to attain the main properties or characteristics. For such a purpose we consider the superpotential defined by $W(h) = h^\sigma/\lambda^2$ and we study the solitons for $\sigma \geq 2$. It is shown the soliton profiles exhibit a compactonlike format for sufficiently large values of the electromagnetic coupling constant g . Further, the soliton solutions carry magnetic flux and possess nonzero total electric charge and, despite of both be proportional to the winding number N , they are nonquantized quantities because the vacuum value a_∞ is a noninteger number [see Eqs. (100) and (101), respectively]. However, it is shown numerically that for sufficiently large values of the electromagnetic coupling g the vacuum value $a_\infty \rightarrow -1$, thus, both the quantities becomes effectively quantized, in accordance with previous investigations [29, 33, 35, 41].

The more remarkable property is the emergence of the flipping of the magnetic field which implies in a localized magnetic flux inversion. This interesting feature emerges due to presence of both the Maxwell and Chern-Simons

terms in the BPS model (16). We emphasize such a feature is absent in the previous investigations of gauged restricted baby Skyrme models with the Maxwell term [41] or the Chern-Simons term [33] solely .

We now are investigating the existence of BPS solitons in a gauged baby Skyrme models into the presence of Lorentz violation. The results will be reported elsewhere.

ACKNOWLEDGMENTS

This study was financed in part by the Coordenação de Aperfeiçoamento de Pessoal de Nível Superior - Brasil (CAPES) - Finance Code 001. We thank also the Conselho Nacional de Desenvolvimento Científico e Tecnológico (CNPq), and the Fundação de Amparo à Pesquisa e ao Desenvolvimento Científico e Tecnológico do Maranhão (FAPEMA) (Brazilian Government agencies). In particular, ACS, CFF and ALM thank the full support from CAPES. RC acknowledges the support from the grants CNPq/306385/2015-5, CNPq/423862/2018-9 and FAPEMA/Universal-01131/17.

-
- [1] T. H. R. Skyrme, Proc. R. Soc. London 260, 127 (1961); Nucl. Phys. 31, 556 (1962); J. Math. Phys. (N.Y.) 12, 1735 (1971).
 - [2] G. Adkins, C. Nappi, and E. Witten, Nucl. Phys. B228, 552 (1983).
 - [3] G. Adkins and C. Nappi, Nucl. Phys. B233, 109 (1984).
 - [4] E. Braaten and L. Carson, Phys. Rev. D 38, 3525 (1988).
 - [5] O.V. Manko, N. S. Manton, and S.W. Wood, Phys. Rev. C 76, 055203 (2007); R.A. Battye, N. S. Manton, P. M. Sutcliffe, and S.W. Wood, Phys. Rev. C 80, 034323 (2009).
 - [6] G.E. Volovik, *Exotic Properties of Superfluid ^3He* , World Scientific (1992).
 - [7] G.E. Volovik, *The Universe in a Helium Droplet* Oxford University Press, New York (2009).
 - [8] S. L. Soundhi, A. Karlhede, S. A. Kivelson, and E. H. Rezayi, Phys. Rev. B 47, 16 419 (1993).
 - [9] S.D. Sarma, A. Pinczuk, *Perspective in Quantum Hall Effects: Novel Quantum Liquids in Low-dimensional Semiconductor Structures*, Wiley, VCH (1996).
 - [10] N.R. Walet and T. Weidig, Europhys. Lett. 55, 633 (2001).
 - [11] Usama Al Khawaja and Henk Stoof, Nature 411, pages 918–920 (2001).
 - [12] Jun-ichi Fukuda and Slobodan Žumer, Nature Communications 2, 246 (2011).
 - [13] S. Mühlbauer, B. Binz, F. Jonietz, C. Pfleiderer, A. Rosch, A. Neubauer, R. Georgii, P. Böni, Science 323, 915 (2009).
 - [14] S.D. Yi, S. Onoda, N. Nagaosa, J.H. Han, Phys. Rev. B 80, 054416 (2009).
 - [15] X.Z. Yu, Y. Onose, N. Kanazawa, J.H. Park, J.H.Han, Y. Matsui, N. Nagaosa, Y. Tokura, Nature 465, 901 (2010).
 - [16] J. Garaud, J. Carlstrom, E. Babaev, and M. Speight, Physical Review B 87, 014507 (2013).
 - [17] J. Garaud, E. Babaev, Scientific Reports 5, 17540, (2015).
 - [18] A. A. Zyuzin, J. Garaud, and E. Babaev, Phys. Rev. Lett. 119, 167001, (2017)
 - [19] T. Winyard, M. Silaev, E. Babaev, Phys. Rev. B 99, 024501 (2019).
 - [20] V. L. Vadimov, M. V. Sapozhnikov, and A. S. Mel'nikov, Appl. Phys. Lett. 113, 032402 (2018).
 - [21] A.N. Bogdanov, A. Hubert, J. Mag. Mag. Mat. 195, 182 (1999).
 - [22] A.N. Bogdanov, U.K. Röbfler, Phys. Rev. Lett. 87, 037203 (2001).
 - [23] A.N. Bogdanov, U.K. Röbfler, M. Wolf, K.H. Müllner, Phys. Rev. B 66, 214410 (2002).
 - [24] U.K. Röbfler, A.N. Bogdanov, C. Pfleiderer, Nature 442, 797 (2006).
 - [25] B. M. A. G. Piette, B. J. Schoers, and W. J. Zakrzewski, Z. Phys. C 65, 165 (1995); Nucl. Phys. B439, 205 (1995); R. B.M.A.G. Piette and W. J. Zakrzewski, Chaos Solitons Fractals 5, 2495 (1995); A. Kudryavtsev, B. M. A. G. Piette, and W. J. Zakrzewski, Eur. Phys. J. C 1, 333 (1998); S. Bolognesi and W. Zakrzewski, Phys. Rev. D 91, 045034 856 (2015).
 - [26] R. A. Leese, M. Peyrard, and W. J. Zakrzewski, Nonlinearity 3, 773 (1990);
 - [27] T. Gisiger and M. B. Paranjape, Phys. Rev. D 55, 7731 (1997).
 - [28] C. Adam, T. Romanczukiewicz, J. Sanchez-Guillen, and A. Wereszczynski, Phys. Rev. D 81, 085007 (2010).
 - [29] J. Gladikowski, B. M. A. G. Piette, and B. J. Schroers, Phys. Rev. D 53, 844 (1996).

- [30] C. Adam, C. Naya, T. Romanczukiewicz, J. Sanchez-Guillen, A. Wereszczynski, JHEP 1505 (2015) 155
- [31] A. Samoilenka and Ya. Shnir, Phys. Rev. D **93**, 065018 (2016).
- [32] A. Samoilenka and Ya. Shnir, Phys. Rev. D **97**, 045004 (2018).
- [33] R. Casana, A. Cavalcante, C. F. Farias and A. L. Mota, Phys. Rev. D **100**, 045022 (2019).
- [34] A. Yu. Loginov, JETP **118**, 217 (2014).
- [35] A. Samoilenka and Ya. Shnir, Phys. Rev. D **95**, 045002 (2017).
- [36] F. Navarro-Lerida and D. H. Tchrakian, Phys. Rev. D **99**, 045007 (2019).
- [37] F. Navarro-Lerida, E. Radu and D. H. Tchrakian, Phys. Lett. B **791**, 287 (2019).
- [38] B. J. Schroers, Phys. Lett. B **356**, 291 (1995).
- [39] P. J. Ghosh, and S. K. Ghosh Phys. Lett. B **366**, 199 (1996).
- [40] C. Lee, K. Lee and H. Min, Phys. Lett. B **252**, 79 (1990).
- [41] C. Adam, C. Naya, J. Sanchez-Guillen, and A. Wereszczynski, Phys. Rev. D **86**, 045010 (2012).
- [42] L. T. Stepien, J. Phys. A **49**, 17, 175202 (2016); J. Phys. A **51**, 015208 (2018).
- [43] C. Adam and A. Wereszczynski, Phys. Rev. D **95**, 116006 (2017).
- [44] S. B. Gudnason, M. Nitta, S. Sasaki. JHEP 1602 (2016) 074
- [45] M. Nitta and S. Sasaki, Phys. Rev. D **91**, 125025 (2015)
- [46] C. Adam, J. M. Queiruga, J. Sanchez-Guillen, A. Wereszczynski, JHEP 1305 (2013) 108.
- [47] C. Adam, J. M. Queiruga, J. Sanchez-Guillen, A. Wereszczynski, JHEP 1907 (2019) 164.
- [48] J. M. Queiruga, J. Phys. A **52**, 055202 (2019).
- [49] M. Wachla, Phys. Rev. D **99**, 065006 (2018).
- [50] R. Rajaraman, *Solitons and Instantons*, North-Holland, Amsterdam (1982).
- [51] C. K. Lee, K. M. Lee, and H. Min, Phys. Lett. B **252**, 79 (1990).
- [52] K. Kimm, K. Lee and T. Lee, Phys. Rev. D **53**, 4436 (1996).
- [53] S. Bolognesi and S. B. Gudnason, Nucl. Phys. **B805**, 104 (2008).
- [54] R. Casana, M. M. Ferreira Jr, E. da Hora and C. Miller, Phys. Lett. B **718** 620 (2012).
- [55] R. Casana and G. Lazar, Phys. Rev. D **90** 065007 (2014).
- [56] R. Casana, C. F. Farias and M. M. Ferreira Jr., Phys. Rev. D **92** 125024 (2015).
- [57] R. Casana, C. F. Farias, M. M. Ferreira Jr. and G. Lazar, Phys. Rev. D **94**, 065036 (2016).
- [58] K. Skenderis and P. K. Townsend, Phys. Lett. B **468**, 46 (1999).
- [59] O. DeWolfe, D. Z. Freedman, S. S. Gubser, and A. Karch, Phys. Rev. D **62**, 046008 (2000).
- [60] M. Trigiante, T. Van Riet, and B. Vercnocke, J. High Energy Phys. **05** (2012) 078.
- [61] E. Megías, G. Nardini, and M. Quirós, J. High Energy Phys. **09** (2018) 095.
- [62] K. Skenderis and P. K. Townsend, Phys. Rev. Lett. **96**, 191301 (2006).
- [63] A. Berera, J. Mabillard, M. Pieroni, and R. O. Ramos, J. Cosmol. Astropart. Phys. **07** (2018) 021.
- [64] F. Cicciarella, J. Mabillard, and M. Pieroni, J. Cosmol. Astropart. Phys. **01** (2018) 024.
- [65] E. Witten and D. Olive, Phys. Lett. B **78**, 97 (1978).
- [66] Z. Hlousek and D. Spector, Nucl. Phys. **B370**, 143 (1992).
- [67] H. Weigel, B. Schwesinger, and G. Holzwarth, Phys. Lett. **168B**, 321 (1986); J. J. M. Verbaarschot et al., Nucl. Phys. **A468**, 520 (1987).
- [68] R. Jackiw, K. Lee and E.J. Weinberg, Phys. Lett. **64** 2234 (1990); Phys. Rev. D **42** 3488 (1990);
- [69] S.K. Paul and A. Khare, Phys. Lett. **B174** 420 (1986).
- [70] H. B. Nielsen and P. Olesen, Nucl. Phys. **B61**, 45 (1973).
- [71] T. Gisiger and M. B. Paranjape, Phys. Rev. D **55**, 7731 (1997).
- [72] E. Babev, J. Jaykka and M. Speight, Phys. Rev. Lett. **103** 237002 (2009).
- [73] R. Casana, M. M. Ferreira Jr., E. da Hora and A. B. F. Neves, Eur. Phys. J. C **74**, 3064 (2014).
- [74] Mohamed M. Anber, Yannis Burnier, Eray Sabancilar, and Mikhail Shaposhnikov, Phys. Rev. D **92**, 085049 (2015).
- [75] R. Casana, A. Cavalcante and E. da Hora. JHEP, **12** (2016) 051 .
- [76] S. K. Paul and A. Khare, Phys. Lett. B **174**, 420 (1986).
- [77] H. J. de Vega and F. A. Schaposnik, Phys. Rev. Lett. **56**, 2564 (1986).
- [78] C. Adam and A. Wereszczynski, Phys. Rev. D **95**, 116006 (2017).
- [79] J. Gladikowski, Z. Phys. C **73** 181 (1996).